Low-energy electron diffraction as a direct identification technique: Atomic structures of Ag- and Li-induced Si(111)-($\sqrt{3}\times\sqrt{3}$)R 30°

H. Over, H. Huang, and S. Y. Tong
Department of Physics and Laboratory for Surface Studies, University of Wisconsin–Milwaukee, Milwaukee, Wisconsin 53201

W. C. Fan and A. Ignatiev
Department of Physics and Space Vacuum Epitaxy Center, University of Houston, Houston, Texas 77204
(Received 14 June 1993; revised manuscript received 18 August 1993)

Quantitative low-energy electron-diffraction (LEED) IV spectra analyses of Ag, Li, and metastable clean ($\sqrt{3}\times\sqrt{3}$)R 30° Si(111) reveal that striking similarities in the LEED spectra are due to common scattering blocks of substrate atoms while the metal atoms are adsorbed at open sites on the Si lattice. This leads to the use of LEED IV spectra as a characterization method. For the ($\sqrt{3}\times\sqrt{3}$)R 30° phases of Li and Ag on Si(111), it is found that both structures can be described by a modified honeycomb-chained-trimer model. The main structural element consists of Si trimers and Si atoms in the deeper reconstructed layers. A counterexample is provided by Si(111)-($\sqrt{3}\times\sqrt{3}$)R 30°-Au for which the IV spectra are very different from those of the other three systems because the common scattering block is absent.

I. INTRODUCTION

Recently, Fan and Ignatiev reported that low-energy electron-diffraction (LEED) IV spectra of the (1×3) phase of Si(111) induced by the adsorption of different metals Ag, Li, and Na showed remarkable similarities.[1] Earlier, striking similarities in the IV spectra have been noted between the metastable clean Si(111)-($\sqrt{3}\times\sqrt{3}$)R 30° phase (hereafter referred to as $\sqrt{3}$-Si) and the Ag covered Si(111)-($\sqrt{3}\times\sqrt{3}$)R 30° phase (Ag-$\sqrt{3}$-Si).[2] The lack of or weak influence of the metal atoms on the IV spectra led to the speculation that the metal atoms must not have a long-range order in these systems. However, such a conclusion is at odds with the findings of many other techniques. On the Ag-$\sqrt{3}$-Si surface, for example, a host of experimental studies, notably ion scattering,[3,4] x-ray diffraction[5,6] and standing wave analysis,[7] reflection high-energy electron diffraction,[8] transmission electron diffraction,[9] scanning tunneling microscopy (STM),[10,11] as well as total-energy calculations[12] supported a model in which the Ag atoms form an essentially flat layer in a honeycomb-chain-trimer (HCT) structure.

In this paper, we propose an alternate explanation for the striking similarities observed in the LEED IV spectra of these systems. We show that IV spectra similarities in the different metal-covered systems are due to the presence of common "scattering blocks" of near neighbor substrate, i.e. Si, atoms. These "scattering blocks" with essentially the same short-range order, produce similar features in the IV spectra, particularly at higher energies for the integral order beams and at all energies for the fractional order beams. Furthermore, to explain the weak influence of the metal atoms on the IV spectra, we propose that the metal atoms are located at "open sites" on the Si lattice providing a pseudo-(1×1) configuration. So, in a kinematic picture single scattering of metal atoms will not contribute strongly to the fractional order beams; the only way for metal atoms to contribute is through a second-order scattering of nearby Si atoms. Because the IV spectra are measured at normal incidence, the strongest scattering path involving a metal atom is between it and the Si atoms directly underneath (dominant forward scattering). A weak influence of the metal atom requires that this metal-Si vertical distance be large. It is immediately clear that this requirement is consistent with the coordination of the Ag atoms in the HCT model. In this model, the Ag atoms are located above sixth-layer Si atoms and the Ag-Si distance is 6.7 Å. To provide quantitative support for this description, we carried out IV spectra analyses based on dynamical LEED calculations. Besides the clean and Ag-covered Si(111)-($\sqrt{3}\times\sqrt{3}$)R 30° phases, we have also determined the structures of Li and Au-($\sqrt{3}\times\sqrt{3}$)R 30° phases on Si(111) (hereafter referred to as Li-$\sqrt{3}$-Si and Au-$\sqrt{3}$-Si, respectively). Qualitatively, the measured IV spectra of the Li-$\sqrt{3}$-Si surface showed great similarities with those of the Ag-$\sqrt{3}$-Si system, while those of the Au-$\sqrt{3}$-Si surface were very different. Using the above reasoning, we expect that in Li-$\sqrt{3}$-Si, the same near-neighbor scattering block of Si atoms exists while the scattering block in the Au-$\sqrt{3}$-Si system is different. As we shall later show, these predictions are confirmed by quantitative IV spectra analyses. The structure of the Au-$\sqrt{3}$-Si surface has been analyzed before by total-energy theory[13] and experiment.[14,15] This is, however, the first time that the Li-$\sqrt{3}$-Si structure is determined. Also, for the first time the Ag-$\sqrt{3}$-Si structure is determined by dynamical LEED analysis to show a result consistent with that of other techniques.

Our use of direct identification (i.e., "fingerprinting") features in LEED is based on the local scattering picture predicted by Yang, Jona, and Marcus[16] and later used by Heinz, Stark, and Bothe[17] to compare major IV features

0163-1829/93/48(20)/15353(5)/$06.00

in LEED and diffuse LEED. In the previous cases, similar scattering blocks involved common adsorbate-substrate clusters. In this work, the "fingerprinting" applied to different adsorbate systems (in order to find a promising starting configuration for the structural refinement of Li-$\sqrt{3}$-Si and to explain the great similarities of IV curves of Li-$\sqrt{3}$-Si with those of Ag-$\sqrt{3}$-Si), requiring that common scattering blocks exist involving only substrate atoms and the adsorbate atoms must locate at open sites on a substrate lattice. A more detailed description of this technique and its applications to overlayer structures on both simiconductor and metal surfaces will be given elsewhere.[18]

II. LEED CALCULATION

The dynamical LEED intensity calculations were performed using the programs of Moritz and co-workers[19] (automated search) and Huang *et al.* (grid search).[20] The former is based on the layer-doubling method and the layer Korringa-Kohn-Rostocker approach[21] while the latter is based on the combined-space method.[22] Both programs extensively exploit symmetry relations in real[23] and reciprocal spaces.[24,25] The two sets of programs produced identical IV spectra on the same systems. The dynamical calculations employed up to nine spin-averaged phase shifts and the atomic scattering matrices were corrected for the effect of dynamical and static disorder using a Debye temperature of 650 K for Si, 450 K for Li, 450 K for Ag, and 450 K for Au; no attempt was made to optimize these parameters. The agreement between experimental and theoretical I-V data was quantified by both the r_{DE} factor introduced by Kleinle *et al.*[26] and Pendry's r_P factor.[27] The experimental I-V curves of Ag-$\sqrt{3}$-Si were analyzed in two stages. First, a dynamical LEED analysis was performed in which only first double layer reconstruction was allowed and the bulk structure was kept in the deeper layers. A coarsely meshed grid search was carried out with structural variations in steps of 0.1 and 0.2 Å for vertical and lateral displacements, respectively. This search enabled us to identify the most promising starting configuration for further structural refinement. In the structural refinement, an extended version of a nonlinear least-squares optimization procedure with respect to intensities as well as to the Y functions[27,19] was applied. Since the formation of Si trimers in the first Si layer is expected to induce distortions in deeper Si layers, we varied up to 12 structural parameters involving full relaxations in the first six layers. This large number of variable parameters cannot be accommodated with standard grid-search techniques but rather requires the application of an automatic optimization scheme.

III. RESULTS AND DISCUSSION

The experimental data comprised five integer and four fractional order beams (in the energy range of 30–250 eV) for Ag-$\sqrt{3}$-Si and Li-$\sqrt{3}$-Si. For clean $\sqrt{3}$-Si and Au-$\sqrt{3}$-Si, two and nine integral, and two and nine fractional order beams, respectively, were used. All the IV spectra were taken at normal incidence and the experimental procedure has been described elsewhere.[1,2,15]

A. Si(111)-($\sqrt{3}\times\sqrt{3}$)R 30°-Ag phase

The automated search for the Ag-$\sqrt{3}$-Si system found that the missing top-layer HCT model produced the best agreement between experiment and theory. This was quantified by the r factors $r_{\mathrm{DE}}=0.38$ and $r_P=0.47$. All other models proposed in the literature[12] could clearly be ruled out; compare Table I. A schematic diagram of the HCT structure is presented in Fig. 1. The multilayer structural parameters are tabulated in Table II, together with comparisons with other techniques. The quoted error bars for LEED assumed a 95% reliability taking into account statistical errors only.[27]

In the HCT model, the Ag atoms replaced the top Si layer (the layer index refers to that of the Si(111) bulk structure, see Fig. 1). The Ag atoms are displaced laterally from bulk sites by 0.59±0.12 Å. The Si atoms in the layer below are displaced by 0.78±0.12 Å to form trimers centered above fourth-layer atoms. The formation of the Si trimers satisfies two of the three dangling bonds while the remaining dangling bond is satisfied by bonding with an Ag atom. The Si trimer formation greatly distorts the substrate lattice and large relaxations down to the sixth atomic layer are present to relieve the strain. A vertical buckling of Si atoms in the fourth and fifth layers of 0.20±0.05 and 0.14±0.07 Å, respectively, and a lateral displacement of Si atoms in the third layer of 0.07±0.04 Å were found in this study. The top interlayer spacing between Ag and Si was found to be 0.69±0.03 Å. The comparison of IV spectra between experiment and theory for the optimal structure are depicted in Fig. 2, left panel, and for reasons of direct compar-

TABLE I. Minimum Pendry R factors for the optimum geometries of various models known from the literature.

Model	Ag coverage	r Pendry
Vacancy model (Ref. 2)	0.00	0.63
Honeycomb model (Ref. 10b)	0.66	0.72
Missing top-layer model (Ref. 30)	0.66	0.68
Embedded trimer model (Ref. 10a)	1.00	0.74
Substitutional trimer model (Ref. 31)	1.00	0.67
HCT full double-layer Si (Ref. 8)	1.00	0.81
Conjugate HCT model (Ref. 13)	1.00	0.71
HCT model (Refs. 12 and 32)	1.00	0.47

TABLE II. Structural parameters by LEED for Si-$\sqrt{3}$-Ag compared with other techniques. Symbols refer to Fig. 1, lengths in Angstroms. RHEED is reflection high-energy electron diffraction, XRD is x-ray diffraction, XSW is x-ray standing-wave analysis, and CAICISS is coaxial impact-collision ion-scattering spectroscopy.

	RHEED (Ref. 8)	XRD (Ref. 5)	XRD (Ref. 6)	XRD/XSW (Ref. 7)	Theory (Ref. 12)	CAICISS (Ref. 4)	LEED (This work)
x_{Ag}	3.06	2.93±0.09		2.86±0.27	2.86		2.80±0.12
Ag-Ag	3.36	3.39	3.43±0.01	3.43	3.45	3.39±0.02	3.45±0.12
Ag-Si		2.54	2.59±0.03	2.57±0.05	2.54	2.61	2.41±0.20
		2.68		2.63±0.06	2.60		
Si-Si	2.7±0.5	2.30	2.31±0.05	2.32±0.04	2.51		2.49±0.10
z_{Ag}	2.95±0.05	2.95±0.10	3.05±0.02	3.05±0.02	3.15	2.9	3.00±0.03
z_{Si}	2.2±0.1	2.1±0.2	2.25±0.02	2.26	2.30		2.31±0.04
z(Ag-Si)	0.75±0.1	0.85±0.2	0.80±0.02	0.8	0.85	0.75±0.07	0.69±0.03
buckled layer 4			0.35±0.05				0.20±0.05
buckled layer 5			0.23±0.04				0.14±0.07

ison, the corresponding IV curves for the other three systems are also shown in this figure. The fractional order beams are shown because they are most sensitive to the scattering block associated with the $\sqrt{3}\times\sqrt{3}$ unit mesh.

Referring to comparison of the structural results found by LEED and those of other techniques (Table II), most of the parameters are in excellent agreement. A noticeable difference is the top Ag-Si interlayer spacing which is about 0.1–0.15 Å shorter in the LEED result. A recent STM study[11] revealed the existence of two registries for the Si trimers. In one domain, the Si trimers were centered above fourth-layer atoms while in the other domain, the Si trimers were centered above sixth-layer atoms. The top layer Ag atoms are correspondingly rotated in the two domains. Our calculations using 100% sixth-layer-centered trimers resulted in poor agreement with the experiment ($r_{DE}=0.60$, $r_P=0.65$); however, mixtures of the two domains led to a slight improvement *as long as the concentration of the sixth-layer-centered trimer domains was less than 30%.*

B. Si(111)-($\sqrt{3}\times\sqrt{3}$)*R* 30°-Li phase

Turning to the Li-$\sqrt{3}$-Si system, their striking similarities in the IV curves to those of Ag-$\sqrt{3}$-Si (as quantified by $r_P=0.45$) suggest that there exists a common scattering block comprising Si atoms. From the Ag-$\sqrt{3}$-Si structure, it is clear that this scattering block consists of second-layer Si trimers and Si atoms in the deeper reconstructed layers. Indeed, dynamical IV spectra analysis corroborated this idea. The structural parameters determined by the automated LEED search are listed in Table III, second column. The Si-Si bond length within the trimer for Li-$\sqrt{3}$-Si was found to be 2.72±0.10 Å, which was longer (i.e., weaker bonds) than that of the Ag-$\sqrt{3}$-Si

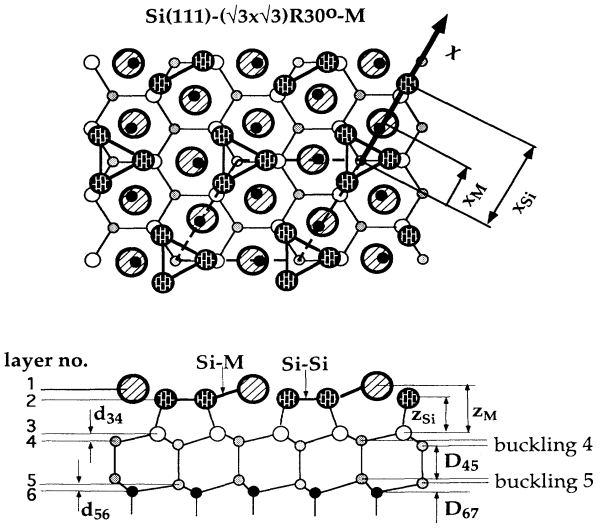

FIG. 1. Schematic view of M-$\sqrt{3}$-Si systems: staggered-shadowing circles represent Si trimers; large circles and hatched circles represent the metal M = Li, Ag, or Au.

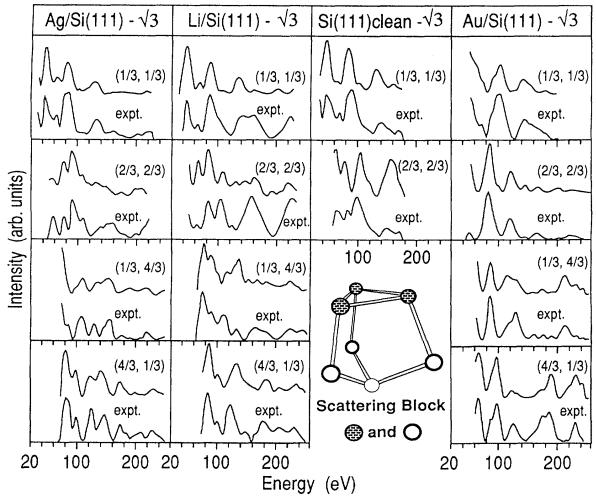

FIG. 2. Comparison of experimental and calculated IV spectra for optimal geometries of Ag, Li, clean and Au-$\sqrt{3}$ systems; Au-$\sqrt{3}$ data from Ref. 15. The inset shows a common Si "scattering block" in Ag-$\sqrt{3}$-Si, Li-$\sqrt{3}$-Si, and $\sqrt{3}$-Si.

TABLE III. Optimal structural parameters for Ag-$\sqrt{3}$-Si, Li-$\sqrt{3}$-Si, $\sqrt{3}$-Si, and Au-$\sqrt{3}$-Si found by LEED. Symbols refer to Fig. 1; M = Ag, Li, Au, lengths in Angstroms.

	Si-$\sqrt{3}$-Ag	Si-$\sqrt{3}$-Li	Si-$\sqrt{3}$-Si	Si-$\sqrt{3}$-Au
x_{Si}	5.21±0.08	5.05±0.08	5.18±0.07	3.92±0.06
x_M	2.80±0.12	2.20±0.10		1.62±0.06
M-M	3.45±0.12	3.84±0.10		2.81±0.06
M-Si	2.41±0.20	2.85±0.14		2.30±0.09
Si-Si	2.49±0.10	2.72±0.10	2.56±0.10	3.48±0.08
z_M	3.00±0.03	2.75±0.03		2.81±0.03
z_{Si}	2.31±0.04	2.30±0.03	2.30±0.03	2.35±0.03
z(M-Si)	0.69±0.03	0.45±0.06		0.46±0.03
buckled layer 4	0.20±0.05	0.18±0.04	0.10±0.04	0.07±0.04
buckled layer 5	0.14±0.07	0.12±0.07	0.05±0.05	0.02±0.04
D_{45}	2.31±0.03	2.30±0.03	2.25±0.03	2.30±0.03
D_{67}	2.21±0.05	2.24±0.05	2.27±0.05	2.31±0.05
d_{34}	0.68±0.03	0.69±0.03	0.72±0.03	0.74±0.03
d_{56}	0.71±0.05	0.73±0.05	0.76±0.04	0.77±0.04

system (2.49±0.10 Å). Also, the Li top-layer atoms are more evenly spaced, i.e., less displaced from bulk positions which is attributed to a stronger dipole-dipole repulsion between Li atoms. An interesting prediction of these structural results is that STM images (none exists to date) might not show honeycomb patterns as observed for the Ag-$\sqrt{3}$-Si system. We thus have the interesting situation wherein the LEED IV spectra for Li- and Ag-$\sqrt{3}$-Si systems are very similar while their STM images might be quite different. The IV spectra comparisons between experiment and theory for the optimal geometry of Li-$\sqrt{3}$-Si are shown in Fig. 2, second column. The r factors are $r_{DE}=0.45$ and $r_P=0.46$.

C. Clean Si(111)-($\sqrt{3}\times\sqrt{3}$)R 30° phase

The clean $\sqrt{3}$-Si system is a metastable structure formed by Ar^+ bombardment followed by rapid annealing (10 K/sec) and rapid cooling (20 K/sec). This structure exists even at room temperature. It was previously analyzed by dynamical LEED and the structure determined was a vacancy model[2] with large vertical inward displacements of top-layer atoms and large lateral displacements of the second-layer atoms. Results of a total-energy calculation[28] showed that a buckling-distortion ($\sqrt{3}\times\sqrt{3}$)R 30° structure is stable on a damaged Si(111) surface with vacancy defects. In this structure, the common scattering block is again a "Si trimer" in the second layer, although these are centered over sixth-layer atoms. Because of the relatively poor long-range order in this system, only limited IV spectra are measurable. The limited data were not sufficient to unambiguously fix the orientation of the trimers. The r factors for the vacancy model are $r_{DE}=0.37$ and $r_P=0.48$, respectively. In this work, we also found a second possible structure in which the trimers are centered over fourth-layer atoms. The top-layer Si atoms occupy near bulk sites with an average concentration of 1 atom/$\sqrt{3}$ unit cell. The structural parameters and the comparisons between experiment and theory for this new model are presented in Table III and Fig. 2, third column. For this model, r_P was improved by 15% but r_{DE} was worsened by 14% from those of the vacancy model.

D. Si(111)-($\sqrt{3}\times\sqrt{3}$)R 30°-Au phase

The experimental IV spectra for the Au-$\sqrt{3}$-Si system are very different from the corresponding data of Ag, Li, and clean systems (see Fig. 2, right column; corresponding r factors are $r_P=0.8$ and $r_P=0.75$, respectively). This structure was solved by Ding, Chan, and Ho[13] using total-energy minimization and the model they proposed was named conjugate honeycomb-chain-trimer (CHCT) with a missing top Si layer. The main features of this model are that the Si atoms in the second layer do not form trimers; instead, Au atoms in the top layer are trimerized which center over fourth-layer atoms. As explained by Ding, Chan, and Ho,[13] this reversal of trimerization from the Ag-$\sqrt{3}$-Si case occurs because the Au-Au bonds are stronger than the Si-Si bonds while the Ag-Ag bonds are the weakest. The table of bond strengths of diatomic molecules[29] indicates that the Si-Si bond with 3.39 eV is stronger than the Ag-Ag bond (1.69 eV), Li-Li bond (1.14 eV), and the Au-Au bond (2.29 eV). Accordingly, the Si-Si interaction dominates in the systems Ag-$\sqrt{3}$-Si and Li-$\sqrt{3}$-Si and drives the structure into HCT configuration. With Au-$\sqrt{3}$-Si the difference in the diatomic bond energies of Au-Au and Si-Si is less pronounced, consistent with the CHCT model found. Quinn, Jona, and Marcus[15] carried out a dynamical LEED analysis of this system which clearly confirmed the CHCT model. Here, we used the data of Quinn, Jona, and Marcus and their structure as our starting configuration for the automatic refinement (of 12 structural parameters). The optimal structural results and the comparisons with Quinn, Jona, and Marcus experiment[15] are shown, respectively, in Table III and Fig. 2, right column. For the optimal structure, $r_{DE}=0.39$ and $r_P=0.35$. Our structural results contain full relaxations of the top six layers which resulted in improvements

in the comparison between experiment and theory. From the structural point of view, the common scattering block of Si trimers and large deeper layer distortions are absent in the Au-$\sqrt{3}$-Si case. A comparison of the IV spectra for Au-$\sqrt{3}$-Si with those of the other three $\sqrt{3}$-Si systems underlines their differences.

IV. CONCLUSION

In conclusion, we have shown that the HCT model for Ag-$\sqrt{3}$-Si is consistent with dynamical LEED analysis and is in agreement with findings of other techniques. In addition, a new surface structure, Li-$\sqrt{3}$-Si, is also shown to have the HCT configuration. Striking similarities in the IV spectra of Ag, Li, and metastable clean $\sqrt{3}$-Si systems support the use of LEED as a direct identification technique. Surface systems having similar IV spectra belong to an equivalent class. Members in the equivalent class are expected to have similar scattering blocks. Therefore, if the structure of any member is solved, its geometric parameters serve as a starting configuration for automated search by dynamical LEED for the other members. The Au-$\sqrt{3}$-Si system offers an interesting counter example and our analysis supports the CHCT model proposed by previous theoretical and experimental studies.

ACKNOWLEDGMENTS

We acknowledge stimulating discussions with J. Nogami and T. Gustafsson. The authors are grateful to F. Jona for providing the experimental LEED I-V data of Au-Si-$\sqrt{3}$. H.O. acknowledges the support of the "Deutsche Forschungsgemeinschaft". Work at Milwaukee was supported by the ONR, Grant No. N000014-90-J1749. Work at Houston was supported by NASA and the R. A. Welch Foundation.

[1]W. C. Fan and A. Ignatiev, Phys. Rev. B **41**, 3592 (1990).
[2]W. C. Fan, A. Ignatiev, H. Huang, and S. Y. Tong, Phys. Rev. Lett. **62**, 1516 (1989).
[3]M. Copel and R. M. Tromp, Phys. Rev. B **39**, 12 688 (1989).
[4]M. Katayama, R. S. Williams, M. Kato, E. Nomura, and M. Aono, Phys. Rev. Lett. **66**, 2762 (1991).
[5]E. Vlieg, E. Fontes, and J. R. Patel, Phys. Rev. B **43**, 7185 (1991).
[6]T. Takahashi and S. Nakatani, Surf. Sci. **282**, 17 (1993).
[7]E. Vlieg, A. W. Denier van der Gon, J. F. van der Veen, J. E. MacDonald, and C. Norris, Surf. Sci. **209**, 100 (1989).
[8]A. Ichimiya, S. Kohmoto, T. Fujii, and Y. Horio, Appl. Surf. Sci. **41/42**, 82 (1989).
[9]Y. Tanishiro, K. Takayanagi, and K. Yagi, Surf. Sci. **258**, L687 (1991).
[10](a) E. J. van Loenen, J. E. Demuth, R. M. Tromp, and R. J. Hamers, Phys. Rev. Lett. **58**, 373 (1987); (b) R. J. Wilson and S. Chiang, *ibid.* **58**, 369 (1987).
[11]K. J. Wan, X. F. Lin, and J. Nogami, Phys. Rev. B **45**, 9509 (1992).
[12]Y. G. Ding, C. T. Chan, and K. M. Ho, Phys. Rev. Lett. **67**, 1454 (1991) and references therein.
[13]Y. G. Ding, C. T. Chan, and K. M. Ho, Surf. Sci. Lett. **275**, L691 (1992).
[14]M. Chester and T. Gustafsson, Surf. Sci. **256**, 135 (1991).
[15]J. Quinn, F. Jona, and P. M. Marcus, Phys. Rev. B **46**, 7288 (1992).
[16]W. S. Yang, F. Jona, and P. M. Marcus, Phys. Rev. B **27**, 1394 (1983).
[17]K. Heinz, U. Starke, and B. Bothe, Surf. Sci. **243**, L70 (1991).
[18]H. Over, M. Gierer, S. Y. Tong, and G. Ertl (unpublished).
[19](a) G. Kleinle, W. Moritz, and G. Ertl, Surf. Sci. **238**, 119 (1990). (b) W. Moritz, H. Over, G. Kleinle, and G. Ertl, in *The Structure of Surfaces III,* edited by S. Y. Tong, M. A. Van Hove, X. Xide, and K. Takayanagi (Springer, Berlin, 1991), p. 128. (c) H. Over, U. Ketterl, W. Moritz, and G. Ertl, Phys. Rev. B **46**, 15 438 (1992). (d) M. Gierer, H. Over, W. Moritz, and G. Ertl (unpublished).
[20]H. Huang, S. Y. Tong, W. E. Packard, and M. B. Webb, Phys. Lett. A **130**, 166 (1988).
[21]J. B. Pendry, *Low Energy Electron Diffraction* (Academic, New York, 1974).
[22]S. Y. Tong and M. A. Van Hove, Phys. Rev. B **16**, 1459 (1977).
[23]W. Moritz, J. Phys. C **17**, 353 (1983).
[24]J. Rundgren and A. Salwen, J. Phys. C **7**, 4247 (1974); **9**, 3701 (1976).
[25]M. A. Van Hove and J. B. Pendry, J. Phys. C **8**, 1362 (1975).
[26]G. Kleinle, W. Moritz, D. L. Adams, and G. Ertl, Surf. Sci. **225**, 171 (1990).
[27]J. B. Pendry, J. Phys. C **13**, 937 (1980).
[28]F. Ancilotto, A. Selloni, and E. Tosatti, Phys. Rev. B **43**, 14 726 (1991).
[29]*CRC Handbook of Chemistry and Physics,* 67th ed., edited by R. C. Weast (CRC, Cleveland, 1986).
[30]S. Kono, K. Higashiyama, T. Kinoshita, T. Miyahara, H. Kato, H. Ohsawa, Y. Enta, F. Maeda, and Y. Yaegashi, Phys. Rev. Lett. **58**, 1555 (1987). E. L. Bullock, G. S. Herman, M. Yamada, D. J. Friedman, and C. S. Fadley, Phys. Rev. B **41**, 1703 (1990).
[31]T. L. Porter, C. S. Chang, and I. S. T. Tsong, Phys. Rev. Lett. **60**, 1739 (1988).
[32]T. Takahashi, S. Nakatani, N. Okamoto, T. Ishikawa, and S. Kikuta, Jpn. J. Appl. Phys. **27**, L573 (1988).